

Abstract Title A Cause for Concern: Causal discovery reveals neoadjuvant radiation leads to increased operative time and blood transfusion in pancreatic cancer

Authors Kelly M. Herremans, MD*; Wenjie Zeng; Andrea N. Riner, MD, MPH; Jordan A. McKean, MD; Daniel W. Neal, MS; Ibrahim Nassour, MD; Panayiotis V. Benos, PhD, Steven J. Hughes, MD

Division of Surgical Oncology, University of Florida Department of Surgery

Abstract.

Introduction: Perioperative blood transfusion is associated with increased 30-day morbidity and mortality as well as overall survival in patients undergoing pancreaticoduodenectomy (PD). As the treatment paradigm shifts toward neoadjuvant therapy in the treatment of pancreatic cancer, little remains known about how this may impact perioperative transfusion rates.

Methods: The American College of Surgeons National Surgical Quality Improvement Project (ACS-NSQIP) database was utilized to identify patients undergoing PD for PDAC from 2014-2019. Patients were divided into groups based on the type of initial treatment they received (neoadjuvant chemoradiation, neoadjuvant chemotherapy, neoadjuvant radiation or surgery first. Univariate analysis (Mann-Whitney and Fisher's exact) and Multivariate (Logistic regression) were performed. Causal discovery was conducted using the rCausalMGM package in RStudio.

Results: A total of 13,404 patients with PDAC underwent PD, with 2745 (20.5%) receiving neoadjuvant chemotherapy only, 154 (1.1%) receiving neoadjuvant radiation only, 1557 (11.6%) receiving neoadjuvant chemoradiation and 8948 (66.8%) undergoing surgery first. Compared to patients who underwent surgery first, those that received neoadjuvant chemoradiation (26.5% vs. 19.2%, $p < 0.0001$), radiation only (31.8 vs. 19.2%, $p = 0.0002$) and chemotherapy only (22.4 vs. 19.2%, $p = 0.0002$) were more likely to receive a blood transfusion intraoperatively or within 72 hours of surgery. Neoadjuvant chemoradiation and radiation alone were independently associated with blood transfusion (OR 1.8 (1.24, 2.63), $p = 0.0004$ and OR 1.3 (1.13, 1.52), $p = 0.002$) based on multivariate analysis. Causal discovery was performed, showing that preoperative radiation leads to increased transfusion rates through increased operative time. Further, transfusion was shown to be independently associated with in-hospital death (OR 3.7 (2.7, 5.13), $p < 0.0001$), discharge destination other than home (OR 2.0 (1.75, 2.25) $p < 0.0001$), complications (OR 1.7 (1.56, 1.88), $p < 0.0001$) and readmission (1.2 (1.04, 1.33), $p < 0.0001$).

Conclusions. Neoadjuvant chemoradiation and neoadjuvant radiation alone are independently associated with perioperative blood transfusion in patients with PDAC undergoing PD. This is likely caused by increased operative times, which may reflect increased difficulty of resection. Future efforts to mitigate the need for perioperative transfusion in these patients is warranted to ultimately reduce the negative short and long-term consequences of perioperative blood transfusion.

Abstract Title: Analysis of 572 Lung Transplants at University of Florida from 2013 to 2023: Characteristics and Outcomes of Orthotopic Single Lung Versus Bilateral Lung Transplant

Authors: Liam Kugler, BS*, Mindaugas Rackauskas, MD, Yuriy Stukov, MD, Griffin Stinson, BS, Ahmet Bilgili, BS, Matthew Purlee, BS, Jin Choi, BS, Anson Wang, BS, Hazel Hutchinson, BS, Kayla Lucas, Omar M. Sharaf, BS, Jeffrey P. Jacobs, MD

Division of Thoracic and Cardiovascular Surgery

Abstract

Introduction: The first human lung transplant was completed on June 11th, 1963. Since then, many advancements have excelled the procedure. We reviewed all 572 lung transplants performed at our institution from 2013 to 2023 and compared characteristics and outcomes of those patients who underwent orthotopic single lung transplant (n= 61) versus patients who underwent bilateral lung transplant (n=511).

Methods: Characteristics and outcomes of patients were compared in all 572 transplants by transplant type. Mann-Whitney tests were used to compare continuous variables and Chi-squared or Fisher’s exact tests were used to compare categorical variables. Kaplan-Meier survival analysis was performed at the level of the patient.

Results: Overall, patients undergoing lung transplant were more likely to be male [Double: n=283 (55.4%); Single: n=47 (77.1%); p=0.001]. Patients undergoing double lung transplant: were younger [Double: 55.8 ± 14.8 years; Single: 68.0 ± 6.1 years; p<0.001], had less body surface area [Double: 1.8 ± 0.3 m2; Single: 1.9 ± 0.3 m2;p=.014], had shorter waitlist time [Double: 63.0 ± 114.6 days; Single: 1247.0 ± 5036.6 days; p=0.027], stayed in the hospital longer [Double: 52.0 ± 59.0 days; Single: 49.6 ± 75.1 days; p=0.005], more likely to survive to discharge [Double: n=493 (95.5%); Single: n=52 (85.3%); p<0.001], more likely to be on iNO/Flolan [Double: n=115 (22.5%); Single: n=6 (10.0%); p=0.025], more likely to be on ECMO pre-transplant [Double: n=64 (12.5%); Single: n=1 (1.7%); p=0.009], and more likely to have post-op complications [Double: n=418 (82.0%); Single: n=40 (65.6%); p=0.002].

Conclusions: Despite sicker pre-transplant status and higher post-op complications, patients who underwent bilateral lung transplant at our institution had improved longitudinal survival compared to patients who underwent single lung transplant.

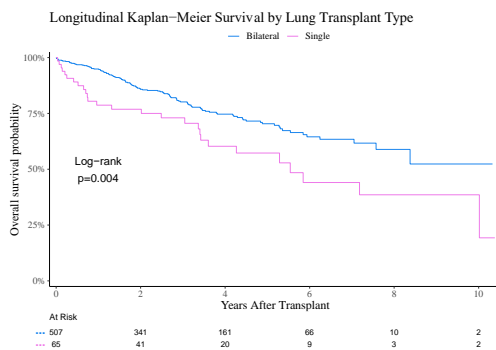


Figure:

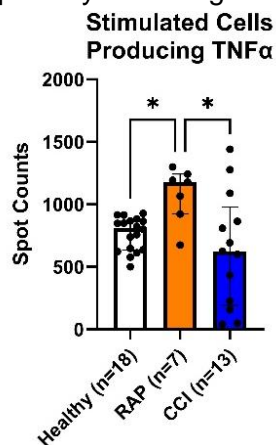
Funding Sources: None

Chronic Critical Illness Induces a Unique Blood Monocytic Response after Sepsis

Evan L. Barrios*, Jaimar Rincon, Valerie E. Polcz, John Leary, Micah Willis, Robert Maile, Lyle L. Moldawer, Rhonda Bacher, Philip A. Efron

Sepsis and Critical Illness Research Center, Department of Surgery, University of Florida

Introduction Chronic critical illness (CCI; ≥ 14 days in ICU, $\text{SOFA} \geq 2$) and rapid recovery have become the predominant outcomes after surgical sepsis. Sepsis survivors with CCI have poor dispositions/increased one-year mortality. We performed Cellular Indexing of Transcriptomes & Epitopes by Sequencing (CITE-Seq) to identify differences in classical ($\text{CD14}^+\text{CD16}^-$) and non-classical ($\text{CD14}^{\text{dim}}\text{CD16}^+$) monocytes between CCI patients and rapidly recoverers to better understand myeloid compartment dysfunction. **Methods** Whole blood and peripheral blood mononuclear cells (PBMCs) were collected from healthy subjects ($n=10-12$) and septic CCI ($n=3-5$) or rapid recovery patients ($n=5-8$). ELISpot was used to determine $\text{TNF}\alpha$ expression via spot counts (cytokine-secreting cells). PBMCs underwent CITEseq and Ingenuity Pathway Analysis (IPA). Cells were annotated and differentially expressed genes (DEGs) were identified via cluster comparison with adjusted p-value < 0.1 . For IPA, enriched canonical pathways were identified via absolute value z-score > 2 and $-\log(\text{p-value})$ greater than 1.3. **Results** ELISpot revealed that septic CCI patients had less cytokine producing cells compared to rapid recoverers (624 spots vs 1177 spots, $p=0.01$) (Fig 1). When comparing CCI vs rapid recovery patients, classical monocytes had 189 downregulated and 185 upregulated DEGs, while non-classical monocytes had 113 downregulated and 53 upregulated DEGs. With regards to IPA, classical monocytes in CCI exhibited downregulated pathways of inflammation (via signaling of IL-6, IL-17, HMBG1, GM-CSF, and LPS-stimulated MAPK) and proliferation (via ERK5, TGF- β , and IL-3 signaling). Upregulated pathways included regulation of inflammatory responses including PPAR signaling & PPAR α /RXR α activation. Non-classical monocytes in CCI exhibited downregulation of pathways including inflammation (signaling of IL-3, PDGF, NGF, Integrin, NOD1/2), migration (G-Protein Coupled Receptor, HGF signaling), and cell proliferation (CXCR4, FLT3, and cAMP-mediated signaling). **Conclusions** Monocytes from septic patients with CCI exhibit chronic dysfunction with a unique transcriptome and immunosuppressive phenotype compared to rapid recovery. This dysfunctional phenotype may be a target for myeloid cell immunotherapeutics in CCI sepsis survivors.



Funding Sources

National Institutes of Health grant RM1 GM139690 (LLM, PAE)

National Institute of General Medical Sciences postgraduate grant T32 GM-008721 (EB, VP)

Abstract Title: Contributors to Postoperative Venous Thromboembolism Risk after Breast Cancer Surgery: A Systematic Review and Meta-Analysis

Authors Syeda Hoorulain Ahmed, MBBS ^{1*}, Ramin Shekouhi, M.D. ¹, Cameron Gerhold, B.S. ², Alexzandra Mattia, B.S. ³, Armina Azizi, M.D. ¹, Gary Donath, M.D. ¹, Harvey Chim, M.D. ¹

¹ Division of Plastic and Reconstructive Surgery, Department of Surgery, University of Florida

² College of Medicine, Florida State University College of Medicine

³ Florida State University College of Medicine, Tallahassee

Abstract.

Introduction: Venous thromboembolism (VTE) events are a preventable complication for patients undergoing surgery for breast cancer. Yet, there is a lack of consistency in the existing literature regarding the potential risk factors affecting these individuals.

Methods: This study aimed to investigate potential risk factors associated with an increased risk of VTE following surgery for breast cancer. Data on patient characteristics such as age, body mass index (BMI), existing comorbidities, smoking history, surgical interventions, duration of hospitalization, and postoperative complications were recorded and analyzed.

Results: Thirty-one studies comprising 22,155 female patients with a mean age of 50.8 ± 2.9 were included. The weighted mean length of surgery and hospital stay was 382.1 ± 170.0 minutes and 4.5 ± 2.7 days, respectively. The patients were followed for a weighted mean duration of 13.8 ± 21.2 months. The total incidence of VTE events was 2.2% (n=489). Meta-analysis showed that patients with postoperative VTE had a significantly higher mean age and BMI, as well as a longer mean length of surgery ($P < 0.05$). Comparing techniques of autologous breast reconstruction showed that the risk of postoperative VTE is significantly higher with deep inferior epigastric perforator (DIEP) flaps ($P < 0.05$). Smoking history, length of hospital stay, and Caprini score did not correlate with increased incidence of postoperative VTE.

Conclusions: The incidence rate of VTE events in patients receiving surgical treatment for breast cancer is 2.2%. Risk factors for developing postoperative VTE in this patient population include older age, increased BMI, extended length of surgical procedures, and DIEP flap reconstruction.

Funding Sources. None

Donor-Recipient Characteristics in Cardiac Transplantation:

Does Donor CPR Affect Longitudinal Survival?

Kelvin Panavelil, Yuriy Stukov, Matthew Purlee, Giles Peek, Mark Bleiweis, Jeffrey Jacobs

Congenital Heart Center, Division of Cardiovascular Surgery, Department of Surgery, University of Florida

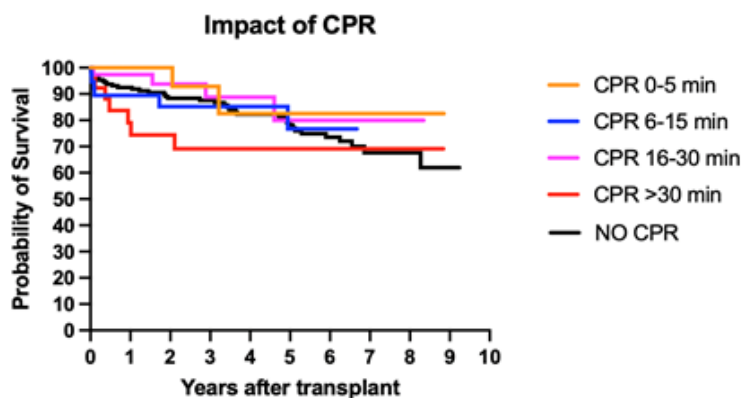
Introduction: Recipient pre-operative variables and their effects on long term survival in cardiac transplantation have been well studied, however donor characteristics are often not addressed in these analyses. We evaluated common donor and recipient characteristics and the impact of CPR on patients' survival.

Methods: 10-year (January 2013- July 2023) retrospective analysis of cardiac donors and recipients at our Center. Continuous variables are presented as median (IQR) while categorical variables are presented as N (%). Donors were divided in 5 groups: no CPR, CPR 5 min, CPR 6-15 min, CPR >16-30 min, CPR >30 min. Kaplan-Meier method was used to estimate longitudinal survival in each cohort.

Results: A total of 359 cardiac donors were included in this study. These donors were split into groups depending on length of CPR. Donors that received more than 30 minutes of CPR were younger, and their matching recipients were more likely to have congenital heart disease. Figure 1 shows Kaplan-Meier estimates for recipient survival. No significant difference in survival for recipients was found regardless of donor CPR administration or length of CPR administered ($p=0.45$).

Conclusions: Longitudinal survival in cardiac transplant recipients is multifactorial and can be influenced by preoperative recipient risk factors as well as donor characteristics such as length of CPR. Statistically not significant trend towards poor outcome was observed in donors with CPR >30 minutes.

Figure 1. Kaplan-Meier Longitudinal Survival Estimates



Abstract Title: Enterococcus hirae Attenuates Pancreatic Cancer Growth Through Activation of Intratumoral Natural Killer Cells

Authors: Angel M. Charles*, Maria Ukhanova, Liang Zhang, Rachel Newsome, Christian Jobin, and Ryan M. Thomas

University of Florida College of Medicine, Department of Surgery, Division of Surgical Oncology
University of Florida College of Medicine, Department of Medicine, Division of Gastroenterology

Abstract:

Introduction: Pancreatic ductal adenocarcinoma (PDAC) is expected to become the 2nd leading cause of cancer-related deaths in the United States by 2030, underscoring the need to better understand mechanisms of pancreatic carcinogenesis. The microbiome, the composite of host microorganisms, has been shown by our lab and others to play a role in PDAC. Previously, we published on the role of the gut microbiome in PDAC via regulation of Natural Killer (NK) cell anti-tumor function. Here we show that intestinal colonization with the bacterium, *Enterococcus hirae* (*Eh*), is able to activate NK cells ex-vivo and reduce PDAC xenograft growth in mouse models via mediating NK cell function in the tumor microenvironment (TME).

Methods: To test the ability of *Eh* to modulate NK cell activity ex-vivo, spleens from C57BL/6J mice were harvested, dissociated into single-cell suspensions and stimulated for six hours with *Eh*-derived cell-free culture supernatant (CFS). Flow cytometry was performed to quantitate the CD45+/CD3-/NK1.1+ NK cell population. *Eh*-derived CFS was used to stimulate the human NK cell line, NK-92mi, *in vitro* for six hours, and interferon gamma (IFN γ) expression was quantified via ELISA (R&D Systems; Minneapolis, MN). To investigate the ability of *Eh* to modulate PDAC anti-tumor immunity *in vivo*, the syngeneic murine PDAC cell line, Pan02, was orthotopically implanted into the pancreas of C57BL/6J mice after 4 days of treatment with broad spectrum antibiotics to deplete the intestinal microbiota. Mice were orally gavaged weekly with 1×10^6 CFU *Eh* (DSMZ; Germany) and colonization confirmed by qPCR of mouse stool. Mice were euthanized four weeks postoperatively, tumors harvested, and tumor weight and volume quantitated. Xenografts were dissociated into single-cell suspensions and flow cytometry was performed to quantitate NK cell population as above, as well as the activated population by IFN γ positivity.

Results: There was a 245% increase in IFN γ expression in C57BL/6J splenic-derived NK cells treated ex-vivo with *Eh* CFS compared to media control ($p < 0.05$). NK-92MI cells treated with *Eh*-derived CFS had a 266% increase in IFN γ expression compared to controls ($p < 0.05$). *In vivo* studies revealed a 53% and 47% reduction in tumor volume and weight, respectively in the xenografts of C57BL/6J mice after treatment with *Eh* vs *E. coli* control ($p = 0.05$ and $p = 0.07$, respectively). NK cell infiltration increased by 59% in *Eh*-treated mice compared to controls ($p = 0.33$), and IFN γ expression increased by 2137% in the intratumoral NK cells from the xenografts of *Eh*-treated mice vs controls ($p < 0.0001$).

Conclusion: *E. hirae* was associated with a reduction in Pan02 PDAC xenograft size *in vivo* and an increase in TME NK cell activation. Studies are ongoing to determine the bacterial products present in the *Eh* CFS responsible for these phenotypes. This study opens the possibility of utilizing bacteria, such as *E. hirae*, to modulate the anti-tumor effect of the host innate immune system in PDAC.

Funding sources: NIH R21, American Cancer Society, University of Florida Cancer Center, University of Florida Department of Surgery

Abstract Title: Human Mesenchymal Stem Cell Extracellular Vesicles Reprogram Immune Signaling Pathways in Burn Patient Immune Cells

Authors Genesis Rodriguez*, Denise A. Hernandez, Madelyn P. Smythe, Micah L. Willis, Matthew F. Warchol, Ian R. Driscoll, Shannon Wallet, Robert Maile

Division of Acute Care Surgery

Abstract

Introduction: Despite clinical advances in patient management, infections are the leading cause of death following burn injury due to dysfunctional immune responses. It is crucial to find a therapeutic that can restore a homeostatic immune response after burn injury. Mesenchymal Stem Cell Derived-Extracellular Vesicles (MSCEVs) have immunomodulatory qualities, and we recently published that MSCEVs are effective in ameliorating overt proinflammatory responses in models of polytrauma. We hypothesized that addition of human MSCEVs to burn patient-derived peripheral blood mononuclear cells (PBMC) would result in significant immune system modulation.

Methods: Bone marrow derived hMSC (ATCC) were cultured to 100% confluency and hMSCEVs purified by ultracentrifugation of supernatant followed by size exclusion chromatography (Izon™). We quantified EV size/concentration by nanotracking analysis (ZetaView). Whole blood was collected from burn patients (n=6, >20% TBSA; <24hrs after injury). PBMCs were isolated, and cultured (4x10⁶ cells/ml) ± 1x10⁶ hMSCEVs/ml. Parallel cultures were set up in the presence of LPS. After 24 hours; supernatant was collected for cytokine analysis (Luminex™) and cell mRNA for immune gene transcriptomics (nanoString™). Data were analyzed using ROSALIND and Ingenuity Pathway Analysis (IPA).

Results: The purification protocol routinely generated 1x10¹⁰/ml EV in 200ml of MSC supernatant, with average diameter of 112nm. When cultured with burn PBMC, in the absence of LPS, hMSCEV induced significant reprogramming of the immune gene transcriptome and secreted cytokines compared to untreated cells. Gene analysis demonstrated significant (**p<0.01) downregulation of 37 immune genes (including IL-32 [0.35 fold change], CD28 [0.5fc]) and upregulation of 46 genes (including CXCL1 [203fc], CCL7 [439fc], IL-19 [68fc], SOCS3 [19fc] and IL-RN [27fc]) in hMSCEV treated versus untreated PBMC. IPA indicated significant (*p<0.05) hMSCEV-reprogramming of immune pathways, including IL-10 Signaling (Z-score=+4.7), macrophage alternative activation (-0.7), IL-17 signaling (+2.8) and wound healing (+1.7) pathways. Cytokine analysis demonstrated a significant upregulation of secreted IL-10 (87fc), IL-1β (387fc), CCL2 (MCP-1; 215fc), IL-6 (2200fc), IL-12p70 (2.2fc) and TNFα (32fc) but not IL-2 or IFNγ after hMSCEV-treatment versus untreated. In the presence of LPS, the only significantly altered genes were IRF3 (1.8fc) and KLRC1 (1.9fc), and MCP-1 was the only cytokine significantly altered (0.6fc).

Conclusions: These data indicate that hMSCEV can reprogram the immune response in ex vivo human burn PBMC collected early after injury. Experiments will determine the 1) ability of hMSCEV to reprogram PBMC collected later after injury; 2) clinically-relevant consequences of this treatment in controlling shock and infection after burn injury

Funding Sources. US ARMY CDMRP BA220315 (Maile)

Abstract Title: Inhibition of Endothelial Cell-Mediated Efferocytosis Promotes Abdominal Aortic Aneurysm Formation

Authors: Jeff Arni C Valisno, Gang Su, Paolo Belotti, Jonathan Krebs, Guoshuai Cai, Guanyi Lu, Ashish K. Sharma, Gilbert R Upchurch Jr.

Vascular Surgery

Introduction: Aortic wall inflammation and aortic smooth muscle (SMC) apoptosis can lead to accumulation of apoptotic cells and debris during abdominal aortic aneurysm (AAA) formation. We hypothesize that dysregulation of MerTK receptor-mediated efferocytosis (clearance of apoptotic cell debris) by endothelial cells (ECs) can significantly contribute to aortic inflammation and vascular remodeling in AAA pathogenesis.

Methods: Single-cell RNA sequencing of human AAA tissue from a published dataset (PMID: 33779682) was evaluated for cells of the aortic wall (SMC/EC) identified via SingleR and cell-specific markers. Differentially expressed genes (DEGs) were identified via edgeR using the QL F-test and efferocytosis-related genes (ERGs) were recognized using a list of 141 ERGs curated from GeneCards. MerTK expression was assessed in human aortic tissue and ECs via western blot and immunofluorescence. Staurosporine-induced apoptotic cells were labelled with PKH67, a green lipophilic dye, and overlaid on ECs labelled with PKH26, a red lipophilic dye, for 45 minutes then washed. ECs were also treated with vehicle, cytochalasin D (a validated inhibitor of efferocytosis; negative control), or UNC5293, a specific inhibitor of MerTK. Efferocytosis was assessed via co-expression of PKH26 and PKH67 in confocal microscopy. Using the established murine elastase AAA model, endothelial-specific MerTK knockout (*Cdh5^{Cre-ERT2}/MerTK^{fl/fl}*) and littermate male mice were analyzed on postoperative day 14 for aortic diameter. Data is presented as mean \pm -SD and Statistical analyses were performed by Welch's T-test where $p < 0.05$ was considered statistically significant.

Results: ERGs (ANXA2, PHACTR1, PPARG, ADAM9, CD14, IL6) were differentially expressed ($p < 0.05$, $\log_2FC > |1|$) between aortic wall cells of human AAAs and control. Human AAA tissue displayed a significant increase in MerTK protein compared to controls (1.51 ± 0.4 vs. 1 ± 0.1 , $n=6/\text{group}$, $p=0.01$). WT ECs displayed robust efferocytosis of apoptotic SMCs compared to negative control ECs treated with cytochalasin D (qualitative data via confocal microscopy). Also, pharmacologic inhibition of MerTK using UNC5293, a specific MerTK inhibitor, attenuated EC-mediated efferocytosis of apoptotic VSMCs (qualitative data; 10 images/group $n=4$). Importantly, EC-specific *MerTK^{-/-}* mice had a significant increase in aortic diameter compared to littermate controls (155 ± 40.4 vs. $103 \pm 30.9\%$, $n=5-6/\text{group}$, $p=0.04$) on day 14.

Conclusion: Our data demonstrates that dysregulation of efferocytosis by ECs regulates AAA formation. Also, aortic ECs mediate efferocytosis of apoptotic SMCs via MerTK to mediate AAA formation. Ongoing studies will delineate mechanisms of MerTK-dependent EC signaling in vascular remodeling during AAA formation.

Funding Sources: NIH R01 HL138931

MerTK-dependent Efferocytosis by Monocytic-MDSCs Mediates Resolution of Post-lung Transplant Injury

Victoria Leroy*, Denny J. Manual Kollareth, Zhenxiao Tu, Jeff Arni C. Valisno, Biplab Saha, Mindaugas Rackauskas, Lyle L. Moldawer, Philip A. Efron, Guoshuai Cai, Carl Atkinson, Gilbert R. Upchurch, Jr., Ashish K. Sharma

Division of Vascular Surgery

Introduction. Lung transplantation (LTx) outcomes are impeded by the development of severe ischemia-reperfusion injury (IRI) which is mediated by dysregulated inflammation-resolution. The reparative role of immunosuppressive immune cells, such as monocytic myeloid-derived suppressor cells (M-MDSCs), remains undescribed in lung IRI. We examined the previously uncharacterized role of MerTK (receptor Mer tyrosine kinase) on M-MDSCs in the process of efferocytosis (clearance of apoptotic cells) to mediate the resolution of post-LTx IRI.

Methods. Single-cell RNA sequencing of post-LTx tissue was analyzed for M-MDSC and MerTK expression using a previously reported dataset (GSE224210). Bronchoalveolar lavage (BAL) from post-LTx patients was analyzed for M-MDSC and soluble Mer protein quantification. Murine lung hilar ligation and allogeneic orthotopic LTx models of IRI were used with Balb/c (WT), *Cebpb*^{-/-} (MDSC-deficient), or *Mertk*^{-/-} mice. IRI was assessed by lung function, inflammation (IL-17A, CXCL1, TNF- α , and IL-6 expression in BAL fluid), and injury (myeloperoxidase expression and immunohistochemistry for neutrophil (PMN) infiltration). Separate groups of WT and *Cebpb*^{-/-} mice were treated with M-MDSCs (5×10^6 cells administered intravenously) 24hrs prior to injury and were subsequently assessed for IRI parameters. *In vivo* and *in vitro* efferocytosis of apoptotic neutrophils by M-MDSCs was assessed via flow cytometry or confocal microscopy. Groups were compared for pairwise comparisons using Mann Whitney test or ANOVA with posthoc Tukey's test, and data is presented as mean \pm standard error of mean.

Results. LTx patients with chronic dysfunction showed a significant downregulation in MerTK-related efferocytosis genes in M-MDSC populations compared to healthy subjects. A significant increase in both M-MDSCs (31.0 ± 6.3 vs. $9.6 \pm 3.5\%$; $p=0.02$; $n=5-7$ /group) and soluble Mer (802.0 ± 142.7 vs. 117.5 ± 29.8 pg/mL; $p<0.0001$; $n=8-10$ /group) was observed in patient BAL post-LTx on day 1 compared to day 0. In the murine IRI model, lung dysfunction, inflammation, and injury were observed after 6hrs in WT mice and were significantly mitigated after 24hrs. This was accompanied by a significant increase in M-MDSCs (12.7 ± 0.6 vs. $5.7 \pm 0.5\%$; $p<0.01$; $n=9-10$ /group), MerTK expression in lung tissue, and M-MDSC efferocytosis of apoptotic PMNs (46.9 ± 1.9 vs. $15.5 \pm 3.2\%$; $p=0.002$; $n=5-8$ /group) after 24hrs compared to 6hrs. However, the resolution of lung IRI was absent in *Cebpb*^{-/-} and *Mertk*^{-/-} mice compared to WT mice at 24hrs, as observed by decreased lung function, increased injury and inflammation, and decreased efferocytosis of PMNs. Adoptive transfer of M-MDSCs derived from WT mice, but not *Mertk*^{-/-} mice, to *Cebpb*^{-/-} mice significantly attenuated lung dysfunction, injury, and inflammation leading to resolution of IRI after 24hrs compared to untreated mice. Additionally, in a preclinical murine orthotopic LTx model, increased M-MDSCs (7.7 ± 1.2 vs. $2.7 \pm 0.4\%$; $p=0.02$, $n=5-6$ /group) were observed following 72hrs reperfusion compared to 24hrs reperfusion which correlated with resolution of lung IRI in recipient mice. Both *in vivo* and *in vitro* studies demonstrated the ability of M-MDSCs to efferocytose apoptotic neutrophils in a MerTK-dependent manner which was analyzed qualitatively and quantitatively via confocal microscopy and flow cytometry, respectively.

Conclusions. Our results demonstrate that M-MDSCs can significantly contribute to the resolution of post-LTx IRI through MerTK-dependent efferocytosis, which is a previously uncharacterized method of immunosuppression by these cells.

Funding Sources. This work was supported by David and Kim Raab Foundation (AKS), National Institute of Health (NIH) F31 HL168827 (VL), and NIH RO1 HL140470-0181 (CA)

Title: Refining a circulating tumor DNA methylation score for HCC detection and cancer progression

Authors: Salar Javanshir Heidari*, Isabella Angeli-Pahim, Sergio Duarte, Ali Zarrinpar.

Division of Transplantation and Hepatobiliary Surgery

Abstract

Introduction: The quantification of methylation patterns of circulating tumor DNA (ctDNA) from plasma samples has shown promise in the noninvasive detection and monitoring of hepatocellular carcinoma (HCC). Previously we used a broad ctDNA tumor methylation score across 550 amplicons in 18 patients with HCC, which demonstrated high specificity and sensitivity in disease detection and progression monitoring. In this study, we aim to refine this scoring system by evaluating a reduced set of amplicons to enhance sensitivity and specificity in HCC detection and disease monitoring.

Methods: 18 subjects were grouped by treatment: resection (5 patients), transplantation (5 patients), Y-90 radioembolization (2 patients), and systemic chemotherapy (6 patients), along with cancer-free controls (4 patients). A total of 101 samples from all patients were studied. New scores were devised using a subset of amplicons selected using varying strategies. Amplicons were categorized based on different selection criteria: *Top 10%* (Amplicons with CpG site methylations scores in the top 10% of at least 5/18 patients), *Most Repeated* (amplicons seen in at least 10/18 patients), *Lowest P-Value* (10 amplicons with the lowest P-value in methylation score between HCC and Healthy patients), *Highest contribution* (10 amplicons with the highest coefficients from logistic regression analysis of HCC patients methylation scores), and *Most Informative* (10 amplicons the omission of which affected the logistic regression analysis most for detection of HCC). For each sample, we generated 5 new tumor methylation scores (TMS) and performed an analysis of each score's ability to distinguish major and minor tumor burden changes as well as monitor disease progression after therapy.

Results: Comparison of the five sets of amplicons revealed significant reductions in scores post-treatment for four out of five groups in patients undergoing resection and transplantation, indicating successful disease eradication. However, the "highest contribution" group failed to show a notable decrease post-treatment. Cancer-free controls had minimal fluctuations in scores from all 5 groups. The refined scoring systems, particularly the amplicons identified in the Top 10% group, exhibited promising specificity for HCC. Change in the top 10% amplicons group methylation scores between longitudinal samples demonstrated an AUC of 0.8958 for distinguishing progression of disease versus no progression (stability or response); This was considerably higher than all other groups and a nearly 10% increase compared to our previous work with the original TMS (0.800). Using the Youden index for the top 10% amplicon TMS as a cutoff, the methylation score from this group had a sensitivity of 83.3% and a specificity of 100%.

Conclusion: The study underscores the potential of circulating tumor DNA methylation analysis as a non-invasive method for HCC diagnosis and monitoring disease progression. These findings have significant implications for clinical practice, offering a valuable tool for early HCC detection and treatment response monitoring. Limitations include the small sample size of HCC patients, warranting validation in larger cohorts. Future research should focus on validating these findings in larger cohorts and exploring their application across different cancer types.

Funding Sources:

None

Title: Risk-Specific Training Cohorts Improve Performance of a Deep Learning Surgical Risk Prediction Model

Authors: Jeremy A. Balch, MD^{1,2}, Timothy R. Buchanan, BS³, Matthew M. Ruppert, MS⁴, Kenneth L. Abbott, MD¹, Benjamin Shickel, PhD⁵, Azra Bihorac, MD, MS⁵, Christopher Tignanelli⁶, Tyler J. Loftus, MD^{1,2}

¹Department of Surgery, University of Florida, Gainesville, FL, USA

²Department of Health Outcomes and Biomedical Informatics, University of Florida, Gainesville, FL, USA

³College of Medicine, University of Florida, Gainesville, FL, USA

⁴College of Medicine, University of Central Florida, Orlando, FL, USA

⁵Department of Medicine, University of Florida, Gainesville, FL, USA

⁶Department of surgery, University of Minnesota, MN, USA

Introduction: Machine learning tools are increasingly deployed in risk prediction algorithms for clinical decision support in surgery. Data imbalance and biases may impact model performance. We hypothesize that model performance will improve when trained on risk-specific cohorts.

Methods: MySurgeryRisk is a deep learning model which generates risk scores for common post-operative complications. Originally trained on all inpatient surgical admissions at single academic hospital over a 7-year period, we subsequently retrained the model on separate cohorts for high-, medium-, and low-risk CPT codes defined by upper-, middle-, and lower-third cut offs for known incidence of 5 complication: in-hospital mortality, prolonged ICU stay \geq 48 hours, prolonged mechanical ventilation \geq 72 hours, sepsis, and acute kidney injury.

Results: 74,800 cases were studied. There were no notable differences between age, BMI, sex, and race between the cohorts. Low-risk CPT codes were defined as having less than 1% and 7% for in-hospital mortality and prolonged ICU stay, respectively, and were defined as 0% for prolonged mechanical ventilation, sepsis, and AKI. High-risk cut offs were 3%, 47%, 8.3%, 4.6%, and 15% for each complication, respectively. While area under the receiver operating characteristic curve (AUROC) had only moderate variance between models, area under the precision-recall curve (AUPRC) and F1 scores were discordant, with high-risk class outperforming the original model and the medium- and low-risk classes in all risk prediction.

Conclusions: When building risk prediction algorithms, predictive performance can be boosted by building separate models for separate risk classes given data imbalance.

Abstract Title: The Effect of Acellular Dermal Matrix Incorporation on Subacute Tissue Expansion

Authors: Sarah A. Applebaum, MD*; Joanna K. Ledwon, PhD; Tianhong Han, BS; Adrian Buganza Tepole, PhD; Arun K. Gosain, MD; Ellen S. Satteson, MD

Division of Plastic and Reconstructive Surgery

Introduction: Acellular dermal matrix (ADM) is used to cover a tissue expander in the prepectoral plane during two-stage tissue expander-based breast reconstruction and is a valuable alternative to total submuscular coverage of the expander. Previous work has demonstrated decreased inflammation and fibrosis of the pocket created by the lining of ADM; however there has been minimal investigation into the role of ADM in skin growth and regeneration induced by the mechanical forces imposed by tissue expansion. The present study evaluates the morphologic and molecular changes mediated by ADM with the goal of improving reconstructive outcomes in women undergoing breast reconstruction with concurrent post-mastectomy radiation therapy. **Methods:** Two tissue expanders, one wrapped in ADM, were placed subcutaneously on bilateral flanks of Yucatan minipigs. All expanders were inflated with two weekly fills of 60cc normal saline and one side of the pig underwent single fraction radiation of 20 Gy. Skin biopsies were harvested after two and ten weeks of expansion from each condition: control, tissue expansion (TE), and tissue expansion with ADM (TE+ADM). Three biopsies per condition were embedded in paraffin or OCT medium and stained with Russell Movat Pentachrome and immunofluorescence (IF) of CD31, respectively. Collagen in the papillary dermis of pentachrome-stained images were analyzed using an ImageJ plug-in, Fibril Tool, that applies circular statistics to estimate average fibril orientation as the direction angle from -90 to 90 with respect to the x-axis. One-way ANOVA evaluated seventy-two measurements per condition and post-hoc analysis with Tukey's HSD test identified significant comparisons between the groups. Number of fluorescent cells expressing CD31 (a marker of endothelial cells) were counted on 12 photographs per condition. P -values $\leq .05$ were considered significant. Total deformation, or skin growth and stretch, was estimated using a computational model and isogeometric analysis. **Results:** The mean fibril orientation of TE and TE+ADM underwent -85% change ($P < .001$) and -15% change ($P = .65$), respectively, compared to control. Three times more CD31⁺ cells were observed in TE+ADM compared to control ($P < .001$), but no significant changes were detected in TE alone. In the presence of ADM, a histogram of total deformation revealed continued growth of expanded skin 2 months after radiation. **Conclusions:** The use of ADM in a porcine model of tissue expansion appears to mitigate disarray of the collagen network in adjacent tissue, thereby creating a more extensive, yet even, distribution of stretched skin and new skin growth. This observation, combined with the finding of increased angiogenesis, suggests it is the incorporation of ADM that confers these protective benefits. Future studies will evaluate molecular changes underpinning the protective role of ADM in compromised tissue beds in order to identify targeted therapy for radiation fibrosis.

Funding Sources: Plastic Surgery Foundation/MTF Biologics Allograft Tissue Research Grant

Abstract Title: Volumetric Analysis of Acute Uncomplicated Type B Aortic Dissection Using an Automated Deep Learning Aortic Zone Segmentation Model

Authors: Jonathan R. Krebs* MD^a, Muhammad Imran PhD^b, Brian Fazzone MD^a, Chelsea Viscardi MD^a, Benjamin Berwick MD^c, Griffin Stinson BS^a, Evans Heithaus MD^c, Gilbert R. Upchurch, Jr. MD^a, Wei Shao PhD^b, Michol A. Cooper MD, PhD^a

^aDepartment of Surgery, Division of Vascular Surgery, University of Florida, Gainesville, FL

^bDepartment of Medicine, University of Florida, Gainesville, FL

^cDepartment of Radiology, University of Florida, Gainesville, FL

Abstract.

Introduction: Machine learning techniques have shown excellent performance in 3D medical image analysis, but have not been applied to acute uncomplicated type B aortic dissection (auTBAD) utilizing SVS/STS-defined aortic zones. The purpose of this study was to establish a trained, automatic machine learning aortic zone segmentation model to facilitate performance of an aortic zone volumetric comparison between auTBAD patients based on rate of aortic growth.

Methods: Patients with auTBAD and serial imaging were identified. For each patient, imaging characteristics from two CT scans were analyzed: (1) the baseline CTA at index admission, and (2) either the most recent surveillance CTA, or the most recent CTA prior to an aortic intervention. Patients were stratified into two comparative groups based on aortic growth: rapid growth (diameter increase ≥ 5 mm/year) and no/slow growth (diameter increase < 5 mm/year). Deidentified images were imported into an open-source software package for medical image analysis and randomly partitioned into training(80%), validation(10%), and testing(10%) cohorts. Training datasets were manually segmented based on SVS/STS criteria. A custom segmentation framework was used to generate the predicted segmentation output and aortic zone volumes. **Results:** Of 59 patients identified for inclusion, rapid growth was observed in 33 (56%) patients and no/slow growth was observed in 26 (44%) patients. There were no differences in baseline demographics, comorbidities, admission mean arterial pressure, number of discharge antihypertensives, or high-risk imaging characteristics between groups ($p > 0.05$ for all). Median duration between baseline and interval CT was 1.07 years (IQR 0.38-2.57). Post-discharge aortic intervention was performed in 13 (22%) of patients at a mean of 1.5 ± 1.2 years, with no difference between groups ($p > 0.05$). In both groups, all zones of the thoracic and abdominal aorta increased in volume over time, with the largest relative increase in Zone 5 with a median 24% increase (IQR 4.4-37). Baseline zone 3 volumes were larger in the no/slow growth ($6v^3$) than the rapid growth group ($5v^3$) ($p = 0.03$). There were no other differences in baseline zone volumes between groups ($p > 0.05$ for all). Dice coefficient, a performance measure of the model output, was 0.73. Performance was best in Zones 4 (0.82), 5(0.88), and 9(0.91). **Conclusions:** To our knowledge this is the first description of an automatic deep learning segmentation model incorporating SVS-defined aortic zones. The open-source, trained model demonstrates high concordance to the manually segmented aortas with the strongest performance in zones 4, 5, and 9, providing a framework for further clinical applications. In our limited sample, there were no differences in baseline aortic zone volumes between rapid growth and no/slow growth patients.